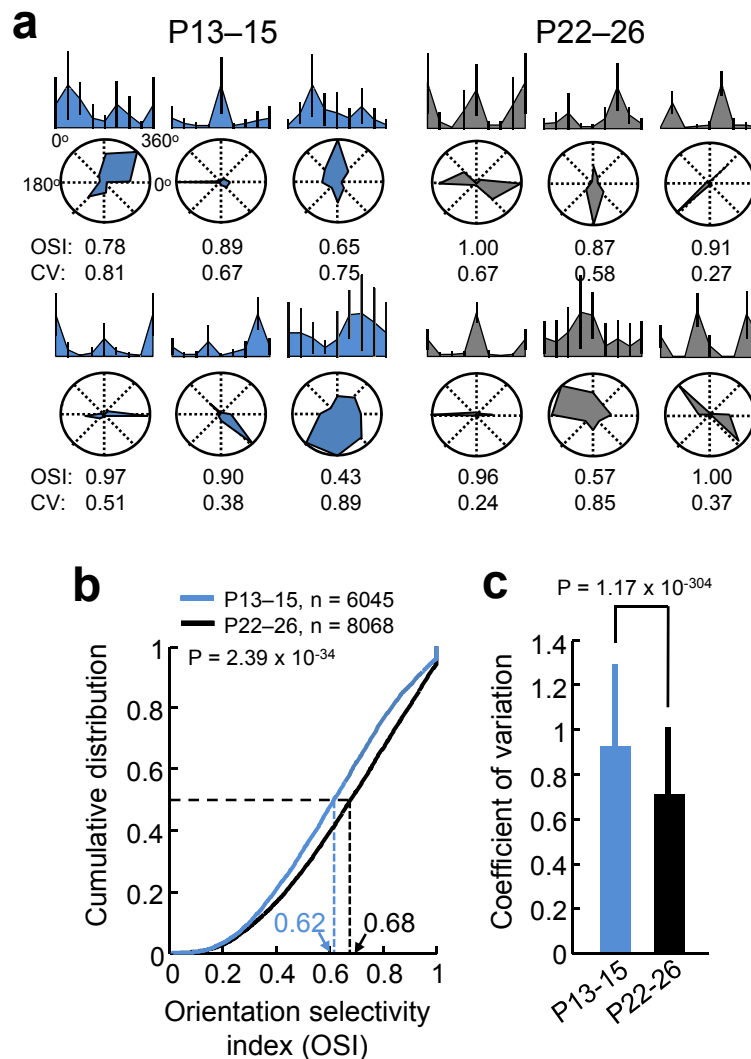


**Supplementary Figure 1. Quantification of RF parameters at eye-opening and with visual experience.**

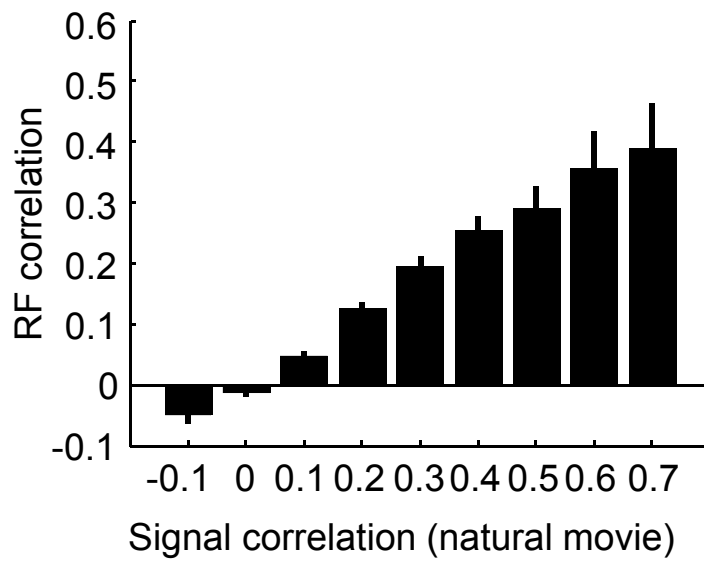
**a**, Example linear RFs at eye-opening (P14–15) and in mature visual cortex

obtained with reverse correlation. Below each RF is the corresponding Gabor fit (see Methods). **b**, Quantification of RF parameters. To obtain a measure of RF size, the visual angles subtended by the Gabor fit along the axes perpendicular ( $\sigma_x$ ) or parallel ( $\sigma_y$ ) to the direction of the cosine grating were calculated (see Methods). To quantify the shape of RFs, we used the dimensionless measures  $n_x = \sigma_x f$  and  $n_y = \sigma_y f$ . These values express the size of the Gaussian envelope in terms of the wavelength of the underlying cosine grating. For instance,  $n_x = 1$  indicates that the standard deviation of the Gaussian perpendicular to the grating is equal to half a cycle of the underlying cosine grating. **c**, Distributions of  $\sigma_x$  and  $\sigma_y$  were not different between immature and more mature V1 (mean visual angle along  $\sigma_x \pm$  s.d., P14 – 15,  $29.3 \pm 13.6^\circ$ ; P28 – 35,  $29.4 \pm 10.3^\circ$ ;  $P = 0.12$ , rank-sum test; mean visual angle along  $\sigma_y \pm$  s.d., P14 – 15,  $19.1 \pm 7.4^\circ$ ; P28 – 35,  $19.9 \pm 7.7^\circ$ ;  $P = 0.25$ , rank-sum test; error bars show s.d.). **d**, Distributions of  $n_x$  and  $n_y$  were not different between immature and more mature V1 (median  $n_x / n_y$ , P14 – 15, 0.31/0.20; P28 – 35, 0.32/0.20;  $P = 0.14/0.41$ , rank-sum test).



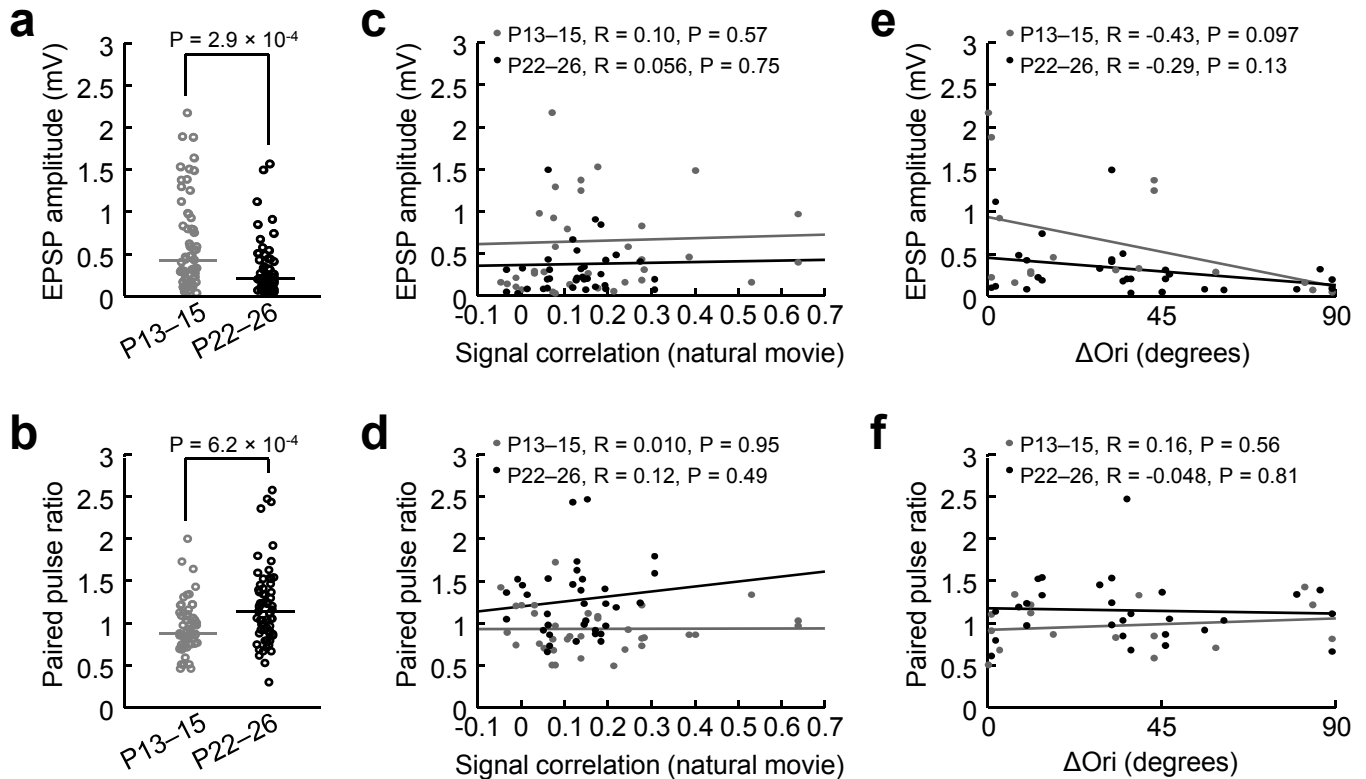
**Supplementary Figure 2. Orientation selectivity and response reliability at eye-opening.**

**a**, Examples of normalized tuning curves (inferred firing rate from calcium signals) and associated polar plots. OSI values were obtained from Fourier fitted tuning curves (see Methods). **b**, Cumulative distribution of orientation selectivity indices (OSI) at eye-opening and in more mature V1 (P13 – 15, median OSI 0.62 vs P 22 – 26, 0.68, P = 2.39 × 10<sup>-34</sup>, rank-sum test). **c**, Coefficient of variation (a measure of trial-to-trial variability, see Methods) of neuronal responses to the preferred grating direction was greater at eye-opening than in more mature V1 (mean CV ± s.d., P13 – 15, : 0.93 ± 0.36 vs P22 – 26, 0.71 ± 0.30, P=1.17 × 10<sup>-304</sup>, rank-sum test; error bars show s.d.). RF data acquired from 4 mice at P14 – 15, and 5 mice at P28 – 35.



**Supplementary Figure 3. Relationship between natural-movie signal correlation and RF correlation.**

Neuronal pairs with higher signal correlations measured from responses to natural movies had higher linear RF correlations. Error bars show s.e.m. Correlation values were binned, with ranges from -0.15 to -0.05, from -0.05 to 0.05, etc.



**Supplementary Figure 4. Relationship between natural-movie signal correlation or difference in preferred orientation and EPSP amplitude and paired-pulse ratio.**

**a**, EPSP amplitudes between L2/3 pyramidal neurons were significantly larger at eye-opening than in more mature V1 (median EPSP amplitude, P13 – 15, 0.41 mV VS P22 – 26, 0.20 mV,  $P = 2.9 \times 10^{-4}$ , rank-sum test). **b**, Paired-pulse ratios between L2/3 pyramidal neurons were significantly lower at eye-opening than in more mature V1 (median PPR, P13 – 15, 0.87, VS P22 – 26, 1.13,  $P = 6.2 \times 10^{-4}$ , rank-sum test). **c**, **d**, There was no correlation between EPSP amplitudes (**c**) or paired-pulse ratio (**d**) and signal correlation at either eye-opening or in more mature V1 ( $P > 0.5$ ). **e**, There was a non-significant trend of decreasing EPSP amplitude with increase in difference in preferred orientation in both age groups (P13 – 15,  $R = -0.43$ ,  $P = 0.097$ ; P22 – 26,  $R = -0.29$ ,  $P = 0.13$ ). **f**, There was no significant correlation between PPR and difference in preferred orientation ( $P > 0.5$  for both groups).